Helium Transport in Flat Vented Divertors and Limiters

H.H. Abou-gabal and G.A. Emmert

July 1989

UWFDM-796

FUSION TECHNOLOGY INSTITUTE

UNIVERSITY OF WISCONSIN

MADISON WISCONSIN

Helium Transport in Flat Vented Divertors and Limiters

H.H. Abou-gabal and G.A. Emmert

Fusion Technology Institute
University of Wisconsin
1500 Engineering Drive
Madison, WI 53706

http://fti.neep.wisc.edu

July 1989

UWFDM-796

Helium Transport in Flat Vented Divertors and Limiters

H.H. Abou-gabal and G.A. Emmert

Fusion Technology Institute
Department of Nuclear Engineering and Engineering Physics
University of Wisconsin–Madison
Madison WI 53706

July 1989

UWFDM-796

Helium Transport in Flat Vented Divertors and Limiters

H. H. Abou-gabal and G.A. Emmert

Fusion Technology Institute

Nuclear Engineering and Engineering Physics Department

University of Wisconsin-Madison

Madison, Wisconsin 53706

The transport of neutral helium atoms near divertor or limiter target plates in fusion devices has been studied using Monte Carlo simulation techniques. The atomic processes of ionization of helium atoms by electron impact and elastic scattering with plasma ions are included. The thermal motion and the streaming of the ions along the magnetic field are also included. Results obtained show significant effects of elastic collisions below about 10 eV, causing a substantial fraction of the helium atoms to be reflected back to the target plate. This effect can be beneficial for the pumping of helium

from the discharge chamber. A two-dimensional Monte Carlo code has been used to study helium recycling near a flat, vented target plate. It is found that a substantial pumping efficiency can be obtained if the transparency of the vented plate is high ($\geq$30%) and the ports are aligned nearly parallel to the magnetic field.

1. Introduction

Helium exhaust is an important problem in the design of magnetic fusion reactors. α particles are produced as a result of the D-T fusion reaction and have to be removed from the system, otherwise the burning fuel will be diluted and the fusion reactivity will be decreased. α particles recombine on a divertor plate or a limiter target and form neutral helium atoms.

Helium atoms generally have a longer mean free path than the neutral hydrogenic species, and therefore penetrate further into the main plasma. This effect can cause helium de-enrichment and make the pumping of helium gas a harder task. As an example, consider a flat vented limiter [1], Fig. 1-a, or a flat vented divertor [2], Fig. 1-b, proposed previously for use in the TIBER-II tokamak. Hydrogenic ions (D^+ and T^+), as well as α particles, following the magnetic field lines in the scrape-off layer hit the divertor plate and get neutralized. If the striking point is inside one of the ports along the plate, the resulting neutral particle can be scattered outside the system and can be driven to the pump duct as shown in Fig. 2 (particle a), otherwise the particle gets scattered towards the plasma (particle b). In the case of hydrogenic species, due to the charge exchange process between the ion and the neutral particle, the latter can return back to the divertor plate where it has a chance to go through one of the ports and into the pump duct. A critical issue for this target plate concept is the pumping of helium. For helium, since we are treating a low temperature regime (below about 40 eV),

the proton-helium charge exchange reaction can be neglected as compared to electron impact ionization and, although charge exchange of helium with He^+ and He^{2+} ions is considerable in the low temperature range, the low density of these ions, as compared to the main plasma density, makes this reaction negligible. Therefore, considering these interactions only, neutral helium has little chance to be backscattered towards the plate unless it gets ionized and returns in the form of an ion. Another interaction which may cause backscattering of the neutral helium to the divertor plate is the elastic scattering of neutral helium by hydrogenic ions. If sufficient backscattering of helium atoms to the plate can be obtained, then pumping of the helium from the system can be accomplished.

Potters and Goedheer [3,4] have considered the elastic scattering process when treating the problem of neutral helium transport in plasmas. Their work is based on a numerical solution of the Boltzmann equation and is restricted to only one-dimensional problems. Since the solution of the Boltzmann equation using the exact form of the elastic collision operator is a rather difficult task, they considered this problem using a simple model (BGK model) in which collisions cause the neutral helium distribution function to relax towards the Maxwellian distribution function at the local temperature, with a relaxation time τ_{He} assumed to be independent of velocity. In other works [5–8], the Monte Carlo method has been used to study helium atom transport, but the process of elastic scattering with ions has not been con-

sidered.

In this work, we consider helium transport in the low temperature plasma edge region. We assume that the neutral helium undergoes either electron impact ionization or elastic scattering on the background ions. A one-dimensional transport code, 1DHET, based on Monte Carlo techniques, has been written to simulate helium atom transport. This allows us to consider the elastic scattering process in a more accurate way and to include the finite flow velocity of the ions with which the helium is colliding. The 1DHET code treats only one-dimensional problems but the use of the Monte Carlo method makes possible its extension to two-dimensional cases, thus becoming the code 2DHET.

In the next section, cross sections for the reactions considered between the helium atoms and the plasma are presented. Section 3 contains the model for wall reflection, while a description of the Monte Carlo simulation is given in section 4. Finally, in sections 5 and 6, numerical applications of the codes and the results obtained are presented. The conclusion of this study are contained in section 7.

2. Plasma-Neutral Helium Interactions

The electron impact ionization rate coefficients for helium are obtained from the formulation of Bell *et al.* [9].

Because of the lack of data on the elastic scattering of neutral helium

by hydrogenic ions, we calculated the needed cross sections using a classical model. Assume a spherically symmetric potential, $V(r)$, with a long range attraction, an attractive well and a short-range repulsion. From elementary considerations of energy and momentum conservation one obtains [10–12] an explicit expression for the classical deflection function, χ,

$$\chi(b,g) = \pi - 2b\int_{r_m}^{\infty} \frac{dr}{r^2}\left[1 - \frac{2V(r)}{\mu g^2} - \left(\frac{b}{r}\right)^2\right]^{-1/2}, \qquad (1)$$

where b is the impact parameter, μ is the reduced mass, g is the initial relative speed of the colliding particles and r_m, the distance of closest approach in the encounter, is the outermost zero of

$$1 - \frac{2V(r_m)}{\mu g^2} - \left(\frac{b}{r_m}\right)^2 = 0.$$

The deflection function χ is positive for net repulsive and negative for net attractive trajectories. The observable scattering angle in the center of mass system is

$$\Theta = |\chi| \quad \text{with} \quad 0 \leq \Theta \leq \pi.$$

Let $\sigma(\Theta, E)$ be the differential elastic scattering cross section where E is the center of mass energy, $E = \frac{1}{2}\mu g^2$. $\sigma(\Theta, E)$ is expressible directly in terms of the deflection function by the relation

$$\sigma(\Theta, E) = \sum_i \frac{b_i}{\sin\Theta}\left|\frac{db}{d\chi}\right|_i, \qquad (2)$$

where the summation is over the various values of b giving rise to the same value of Θ.

The total elastic scattering cross section, σ_s, is defined as

$$\sigma_s(E) = 2\pi \int_0^\infty \sigma(\Theta, E) \sin\Theta \, d\Theta. \tag{3}$$

For the form of $V(r)$, we utilize the results of ab initio calculations by Wolniewicz [13] in which he calculated adiabatic values for the intermolecular potential of the molecular ion HeH^+. Helbig, Millis and Todd [14] have fit these calculations to the following analytical function

$$\begin{aligned} V(r) &= \frac{2}{r} e^{-r/A} \left[1 + \frac{r}{A} + \frac{1}{2} r^2 \left(\frac{1}{A^2} - \frac{U}{B} \right) \right] \\ &\quad - U \left[1 + \frac{r}{B} + (\frac{r}{C})^2 + \frac{2Ur^4}{\alpha} \right]^{-1}, \end{aligned}$$

where U, the difference between the ground-state energies of He and Li^+, equals 4.37311 hartrees (1 hartree = 27.2097 eV), α, the polarizability of He, equals 1.3835 bohr (1 bohr = 0.52917×10^{-8} cm), $A = 0.442$, $B = 0.505$, and $C = 0.451$.

This form of $V(r)$ is plotted in Fig. 3. Differential elastic scattering cross sections at different values of E have been calculated and some of them have been compared to the results of Helbig *et al.* [14]. In Fig. 4, the classical deflection function is plotted versus the impact parameter for $E = 5.79567$ eV. Fig. 5 shows the corresponding classical differential elastic scattering cross section versus Θ. As shown in the figure, our curve is in good agreement with the Helbig *et al.* results. The total elastic scattering cross section is presented in Fig. 6 versus the helium-proton relative speed, g.

The elastic scattering rate coefficient $< \sigma \cdot v >_s$ is given by

$$< \sigma \cdot v >_s = \int \sigma_s(g)\ |\overline{v}_p - \overline{V}|\ f_i(\overline{V})\ d\overline{V}, \tag{4}$$

where $\sigma_s(g)$ is the elastic scattering cross section as a function of the relative speed g, $g = |\overline{v}_p - \overline{V}|$, $\overline{v}_p$ is the velocity of the neutral helium particle, $\overline{V}$ is the ion velocity and $f_i(\overline{V})$ is the ion distribution function.

Since numerical integration of Eq. (4) at each flight of the tracked particle is out of the question, an approximate solution has been introduced [6]. The relative speed g has been substituted with an average speed g^* which is in some way representative of the velocity population. In particular, to simplify the calculations, let

$$g^* = < g^2 >^{1/2},$$

with

$$< g^2 > = \int g^2\ f_i(\overline{V})\ d\overline{V}.$$

For $f_i(\overline{V})$ equal to a shifted Maxwellian,

$$f_i(\overline{V}) = \left(\frac{m_H}{2\pi k T_i}\right)^{1/2} \exp\left[-\frac{m_H}{2kT_i}(\overline{V} - \overline{a})^2\right], \tag{5}$$

where m_H is the mass of the hydrogenic ion, T_i and $\overline{a}$ are the ion temperature and the ion flow velocity respectively, we have [6]

$$g^* = \left[\frac{3kT_i}{m_H} + |\overline{a} - \overline{v}_p|^2\right]^{1/2}.$$

Eq. (4) is then written as

$$< \sigma \cdot v >_s = \sigma_s(g^*)\ g^*.$$

3. Wall Interactions

In this section, the modelling of the interactions of ions and neutrals with divertor or limiter target plates will be described. In a steady state condition, plasma ions hitting a wall or a plate are neutralized and return back to the plasma as a result of mainly two processes: backscattering and re-emission.

Particles of energy E_0 bombarding a surface of a solid at an angle of incidence, α, relative to the surface normal, penetrate for a short distance into the solid and are backscattered (predominantly) as neutrals to the surface with a probability R_N, which is a function of E_0 and α. R_N is called the particle reflection coefficient and defined as the average number of particles backscattered per incident particle. The reflected energy is expressed as a fraction $R_E(E_o, \alpha)$ of the incident energy. The coefficient R_E is called the energy reflection coefficient. Therefore, the mean energy of the backscattered particles $\bar{E}(E_o, \alpha)$ is a result of these definitions

$$\bar{E}(E_o, \alpha) = E_o \frac{R_E(E_o, \alpha)}{R_N(E_o, \alpha)}. \tag{6}$$

Particle and energy reflection coefficients depend further on the solid material and the incident particle.

In many publications, backscattering data are represented not as a function of the incident energy but as a function of the reduced energy, ε, intro-

duced by Lindhard *et al.* [15] and given by

$$\varepsilon = 32.55 \left(\frac{m_1}{m_1 + m_2}\right) \frac{1}{Z_1 Z_2 \left(Z_1^{2/3} + Z_2^{2/3}\right)^{1/2}} E_0,$$

with E_0 in keV and m_1, Z_1, m_2, Z_2 being the mass and nuclear charge of the incident particles and target atoms. The use of ε instead of the actual energy E_0 allows one to scale approximately the backscattering data for different ion-target combinations as long as $m_2 >> m_1$.

In our model, we adopted the forms of the reflection coefficients used by Cupini *et al.* [6]. The coefficient R_N increases with the angle of incidence, α, and approaches 1 for grazing incidence. To account for this, the following formula has been used

$$R_N(E_o, \alpha) = [R_N(E_o) - 1] \cos \alpha + 1,$$

where $R_N(E_o, \alpha)$ is the particle reflection coefficient for non-normal incidence, and $R_N(E_o)$ is the particle reflection coefficient for normal incidence. Since there is a lack of agreement between theoretical and experimental data for the dependence of the energy reflection coefficient on the incidence angle [16,17], any dependence of R_E on α has been neglected in our model.

Therefore, when a particle history reaches a wall the event of backscattering is chosen with probability R_N and the energy of the reflected particle is determined from Eq. (6). As for the angle of the emerging particle, its distribution is reasonably approximated by a cosine law [16], together with a uniformly distributed azimuthal angle. Particles which are not backscattered

slow down to thermal energies and are re-emitted with a speed chosen from a speed Maxwellian distribution

$$f(v) = 4\pi \left(\frac{m_{He}}{2\pi k T_w}\right)^{3/2} v^2 \exp\left[-\frac{m_{He}}{2kT_w} v^2\right], \tag{7}$$

where T_w is the wall temperature and k is the Boltzmann constant. The angles of the re-emitted particle are chosen as in the case of backscattering.

4. Monte Carlo Simulation

In subsection 4.1 a description of the 1DHET code, which treats one-dimensional problems, is presented while subsection 4.2 presents the description of the two-dimensional code, 2DHET.

4.1. One-Dimensional Monte Carlo Code

The geometry of the problem considered and the coordinates used are shown in Fig. 7. The region of interest has a width of z_{max} and is divided into zones of uniform plasma parameters. For the 1-D code the port at $z_{min} < z < 0$ is not present and the plate at $z = 0$ is continuous. The plasma parameters, such as the electron temperature, T_e, the ion temperature, T_i, the plasma density, n_p, the ion flow velocity, $\bar{a}$, and the sheath and pre-sheath potential, Φ, are kept constant during the Monte Carlo calculation.

4.1.1. *Sampling of the Neutral Source Particle*

The code allows the performance of two distinct calculations:

- The first calculation assumes a monoenergetic source of neutral helium particles placed at the target plate. It also assumes that the reflection at the plate is neglected, *i.e.,* when a helium atom leaving the plasma strikes the plate, it will be considered lost from the system. This calculation allows us to obtain the probability for a helium atom born at the target plate to be scattered by the plasma back to the plate because of elastic scattering with plasma ions.

- In the second calculation, the neutral helium source is due to the neutralization of the helium ions incident on the plate. These ions get reflected as neutral helium, as described in section 3. In this case the reflection at the plate is taken into account, *i.e.,* helium atoms striking the plate are allowed to get reflected back as in section 3.

For the second type of calculation, the neutral source particle has its energy obtained as follows:

- An α particle incident on the target plate has its velocity, $\overline{v}_i$, chosen from a shifted Maxwellian distribution

$$f(\overline{v}_i) = \left(\frac{m_{He}}{2\pi k T_{i1}}\right)^{1/2} \exp\left[-\frac{m_{He}}{2kT_{i1}}(\overline{v}_i - \overline{a}_1)^2\right],$$

where T_{i1} is the edge ion temperature and $\overline{a}_1$ is the edge ion flow velocity.

- Because the α particle is accelerated through the sheath potential, Φ, it will therefore have a total incident energy E_o given by

$$E_o = \frac{1}{2} m_{He} v_i^2 + 2\Phi,$$

and it is assumed to be incident normal to the plate.

- Using the reflection model described in section 3, the reflected helium atom will have its velocity $\overline{v}_p$ specified.

4.1.2. Sampling of the Collision

The path length estimator technique [18,19] is used to track the helium particle until a collision point is obtained. As mentioned before, at the collision point the neutral helium atom can either be ionized by electrons or elastically scattered by background ions. Ionization is sampled by using the method of suppression of absorption [6,7,19].

The elastic scattering is treated as follows:

1. The target ion has its velocity, $\overline{V}$, sampled from a shifted Maxwellian distribution given by Eq. (5).

2. Since the collision problem is more easily treated when one particle is at rest, we transform our problem to the frame where the target ion is

at rest. In this frame, frame no. 2, the helium atom will have a velocity $\overline{v}_r$ given by

$$\overline{v}_r = \overline{v}_p - \overline{V},$$

and an energy obtained as

$$E_r = \frac{1}{2}\, m_{He}\, v_r^2.$$

3. A transformation to a center of mass (COM) frame is then performed with the velocity of the center of mass obtained as $\overline{v}_{CM} = \frac{m_{He}}{m_{He}+m_H}\overline{v}_r$.

4. Since the scattering is anisotropic, the scattering angle in the COM frame, Θ, will be sampled using a method employed in the transport of neutrons [20]. This method can be devised by tabulating, for specific incident energies, the $(n+1)$ center-of-mass angles that correspond to n equally probable intervals of the cumulative distribution function, P_i, where P_i is given by

$$P_i = 2\pi \int_{-1}^{(\cos\Theta)_i} \frac{\sigma(\Theta, E_r)}{\sigma_s(E_r)}\, d(\cos\Theta) \qquad i = 0, 1, 2, \ldots, n.$$

Here n is the number of equally likely intervals, set equal to 32 in our calculation, $\sigma(\Theta, E_r)$ is the differential elastic scattering cross section and $\sigma_s(E_r)$ is the total elastic scattering cross section. Our model contains such tables for 30 values of the incident energy E_r. The scattering angle, Θ, is then determined by linear interpolation between consecutive tables.

5. The scattering angle in frame no. 2, θ_2, is then found from

$$\cos\theta_2 = \frac{1 + A\cos\Theta}{(1 + 2A\cos\Theta + A^2)^{1/2}},$$

where $A = m_H/m_{He}$. The speed of the emerging helium atom in frame no. 2, v_r', can be calculated using

$$v_r' = v_r \frac{(1 + A^2 + 2A\cos\Theta)^{1/2}}{1 + A}.$$

The direction cosines of the emerging helium atom in frame no. 2 result from the following equations [21]

$$\text{if} \quad |\omega_{rz}| < 0.999999,$$

$$\begin{aligned}
\omega_{rx}' &= \frac{\sin\theta_2}{\sqrt{1-\omega_{rz}^2}}[\omega_{rx}\omega_{rz}\cos\varphi - \omega_{ry}d] + \omega_{rx}\cos\theta_2, \\
\omega_{ry}' &= \frac{\sin\theta_2}{\sqrt{1-\omega_{rz}^2}}[\omega_{ry}\omega_{rz}\cos\varphi + \omega_{rx}d] + \omega_{ry}\cos\theta_2, \\
\omega_{rz}' &= -\sqrt{1-\omega_{rz}^2}\sin\theta_2\cos\varphi + \cos\theta_2\omega_{rz}.
\end{aligned}$$

Otherwise,

$$\begin{aligned}
\omega_{rx}' &= \sin\theta_2\cos\varphi, \\
\omega_{ry}' &= d\sin\theta_2, \\
\omega_{rz}' &= \omega_{rz}\cos\theta_2.
\end{aligned}$$

The azimuthal angle φ is sampled isotropically from

$$\varphi = \pi(2\xi - 1),$$

where ξ is a random number uniformly distributed between 0 and 1. d is given by

$$d = \begin{cases} -\sin\varphi & \varphi < 0 \\ \sin\varphi & \varphi \geq 0. \end{cases}$$

6. Transforming back to our initial frame, we have the velocity of the scattered helium atom as

$$\begin{aligned} \overline{v'}_p &= \overline{v'}_r + \overline{V}, \\ &= (v_r'\omega_{rx}' + V_x)\hat{x} + (v_r'\omega_{ry}' + V_y)\hat{y} + (v_r'\omega_{rz}' + V_z)\hat{z}, \end{aligned}$$

which can be written as

$$\overline{v'}_p = v_{px}'\hat{x} + v_{py}'\hat{y} + v_{pz}'\hat{z},$$

from which the speed and the direction cosines of the scattered helium atom are calculated by

$$\begin{aligned} v_p' &= (v_{px}'^2 + v_{py}'^2 + v_{pz}'^2)^{1/2}, \\ \omega_x' &= \left[1 - (\frac{v_{pz}'}{v_p'})^2\right]^{1/2} \frac{v_{px}'}{[v_{px}'^2 + v_{py}'^2]^{1/2}}, \\ \omega_y' &= \left[1 - (\frac{v_{pz}'}{v_p'})^2\right]^{1/2} \frac{v_{py}'}{[v_{px}'^2 + v_{py}'^2]^{1/2}}, \\ \omega_z' &= \frac{v_{pz}'}{v_p'}. \end{aligned}$$

The scattered helium atom is then tracked until the particle either escapes from the system or is ionized. A new particle is then launched at the plate and all the above steps are repeated again.

4.2. *Two-Dimensional Monte Carlo Code*

Because we can assume symmetry, only one port with its surrounding region is considered in the 2DHET code. The geometry and the sets of coordinates used are shown in Fig. 7. In this case, we consider the port at $z_{min} < z < 0$. The plasma parameters can vary only in the z direction and are uniform in the x and y directions. In the edge region, a helium atom is assumed to interact with the plasma either by electron impact ionization or by elastic scattering on hydrogenic ions, as in the 1DHET code. Once inside the port, because the interaction mean free path is long compared to the port width, the helium atom is assumed to bounce between the port sides without any collision with the plasma.

The source helium atom is obtained from the neutralization and reflection of the α particles incident on the plate. The sampling steps are similar to those in the 1DHET code except that an x position has to be determined. x is assumed to have a uniform distribution between 0 and $x = x_2$. If

$$x_3 < x < x_4,$$

the α particle will be neutralized on the sides of the port; otherwise, the source helium atom has its parameters obtained exactly as for the second type of source in subsection 4.1.1 and it is directed towards the edge plasma region. In the plasma region, sampling of the collision event is performed in the same manner as in the 1DHET code. In addition, the x coordinate is taken into account. Because of symmetry, if a helium atom leaves the

region across the surfaces $x = 0$ or $x = x_2$, another helium atom enters the region through the opposite surface at the same value of z and with the same velocity and weight as the leaving particle.

If a helium atom, scattered back by the plasma ions to the target plate, enters the port, its collision point with the port sides is determined from the intersections of its trajectory, given by

$$\overline{r} = \overline{r}_o + \overline{v}\,(t - t_o),$$

and the equations $F_i(x, y, z) = 0$ $(i = 1, 2)$, of the port sides. Here $\overline{r}(t)$ is the particle position at time t, $\overline{r}_o$ the initial position (at $t = t_o$) and $\overline{v}$ is the particle velocity. The port sides can be presented by straight lines which are written as

$$F_1(x, y, z) = x - x_3 + z \cot \theta_w = 0 \tag{8}$$

for the lower side, and

$$F_2(x, y, z) = x - x_4 + z \cot \theta_w = 0 \tag{9}$$

for the upper side. Therefore, the collision point is obtained from the solution of either Eq. (8) or Eq. (9) and

$$\frac{x - x_o}{v_x} = \frac{y - y_o}{v_y} = \frac{z - z_o}{v_z} = t - t_o.$$

It is worth noting that the dimension along the y axis enters the problem only in the computation of v as $|\overline{v}| = (v_x^2 + v_y^2 + v_z^2)^{1/2}$. If the helium atom inside the port has a value of z less than z_{min}, the particle is considered lost to the pump and its life ends.

5. One-Dimensional Results

The 1DHET code allows the calculation of the neutral helium density profile and the helium current outgoing from the plasma to the plate, because of elastic scattering. One can also obtain the energy spectrum of the neutral helium at the plate.

A parametric study has been performed to examine the dependence of the helium current outgoing to the plate on the plasma temperature. We assume a hydrogen plasma with uniform and equal electron and ion temperatures in a region of maximum width $z_{max} = 7$ cm. The plasma has a uniform density set equal to $1 \times 10^{14}\,\mathrm{cm}^{-3}$. The values of the plasma density and z_{max} are unimportant as long as the product is large enough such that few helium atoms escape through the boundary at z_{max}. Ions and electrons follow magnetic field lines which are at an angle of 10° to the target plate, which is taken to be iron. The sheath potential, Φ, is assumed to be equal to $3T_e$. The number of helium particles tracked is 10,000.

Two different calculations have been done. The first considers only the emission of 0.05 eV atoms at the plate and their reflection by elastic scattering with the ions. The second calculation considers helium ions incident on the plate, their backscattering and re-emission as atoms, and also backscattering or re-emission when helium atoms strike the plate.

In the first case the atoms are emitted with an energy of 0.05 eV at the target plate. Fig. 8 shows the neutral helium current scattered by the

plasma back to the plate versus the plasma temperature. Since this current is normalized to 1 source particle/cm^2 s, it represents the probability that a 0.05 eV atom born at the plate will be elastically scattered by the ions back to the plate. As shown in Fig. 8, this probability increases as the ion temperature decreases and becomes significant below 10 eV. The low reflection probability of the plasma above 10 eV is because electron impact ionization rises rapidly with electron temperature and becomes dominant above 10 eV.

The second calculation is for neutral helium atoms resulting from the neutralization and reflection of α particles incident on the plate. Fig. 8 shows the helium atom current reflected by the plasma by elastic scattering with ions versus the plasma temperature. As can be seen, the helium current follows the same behavior as in the first case, but the helium current is somewhat lower in this case. This is because most of the neutral atoms arising from the neutralization of α particles are more energetic than the 0.05 eV atoms considered in the first case. These energetic particles penetrate further into the plasma before being scattered or ionized. Those atoms which are scattered back toward the plate by elastic scattering with ions have a greater probability of being ionized before returning to the plate. Fig. 9 shows the neutral helium density versus the distance normal to the target plate, for a plasma with uniform temperature equal to 4 eV. The values of the density shown in the figure are normalized to the flux of the α particles incident on the plate. As can be seen from the figure, the neutral helium has an average

mean free path of about 2 cm. This limits its importance to only a few centimeters from the plate.

6. Two-Dimensional Results

The 2DHET code has been used to study the transport of neutral helium near a flat, vented target plate. We consider a hydrogen plasma with a small amount of α particles and perform a parametric study to examine the effect of various plasma parameters and geometric aspects on the scattering of helium atoms by the plasma back to the target plate and the resulting pumping efficiency. In all the following calculations, we assume that electron and ion temperatures are uniform and equal in the region simulated. The region simulated represents the plasma just in front of the vented target plates shown in Fig. 1. For high density, as in a high recycling divertor, the helium mean free path is small and a slab model with uniform density and temperature is a reasonable approximation. Ions and electrons follow magnetic field lines which are at an angle to the target plate. The plate is taken to be iron with a temperature equal to 0.05 eV. The sheath potential, Φ, is assumed to be equal to $3\,T_e$. The number of helium particles tracked is always set equal to 10,000 particles.

In the following, J_w is defined as the neutral helium current incident on the target plate normalized to one source particle/cm^2 s. J_D is defined as the neutral helium current entering the pump duct normalized to one source

particle/cm^2 s and is an indicator of the pumping efficiency. In the next subsection, the geometric effects are presented while, in subsection 6.2, the effects of the plasma parameters are shown.

6.1. Dependence on Geometric Aspects

We consider the dependence of the two currents on the quantities F_A, which is the ratio of the port area to the plate area, L_p, θ_w, and the angle, β, between the magnetic field lines and the target plate. The geometry is illustrated in Fig. 7. In the calculations, we assume a plasma density equal to 1×10^{14}cm^{-3} and a plasma temperature equal to 4 eV, with equal electron and ion temperatures. The ion flow speed, a, is taken equal to the hydrogen ion sound speed corresponding to the plasma temperature considered, namely,

$$a = \left(\frac{T_e + 3\,T_i}{m_H}\right)^{1/2},$$

where m_H is the hydrogen mass.

J_w is found to be almost independent of all the geometric parameters considered except the angle β between the plate and the magnetic field; it increases as β increases, as shown in Fig. 10. This can be explained by the effect of the angle β on the streaming motion of the ions. As β increases, the component of the ion flow velocity perpendicular to the plate increases. In an elastic scattering interaction, the target hydrogenic ion with a larger perpendicular velocity component causes the interacting helium atom to be backscattered more towards the plate, increasing the value of J_w. It will be

shown in subsection 6.2 that J_w depends on the quantity $a \sin \beta$, which is the perpendicular component of the velocity.

On the other hand, the current, J_D, to the pump duct is found to depend strongly on the geometric aspects considered. Fig. 11 shows an increase in the current J_D as F_A increases. This is due to the fact that by increasing F_A, the transparency of the plate to the incident particles (α particles or backscattered helium atoms) increases, causing more particles to enter the ports. On the contrary, an increase in the port length, L_p, leads to a decrease in the current J_D, as can be seen in Fig. 12. Longer ports cause more collisions for the helium atoms with the port sides which increases the probability for the atoms to return back to the plasma region. Therefore, ports as short and wide as the engineering restrictions allow are beneficial to the pumping of neutral helium. As shown in Fig. 13, J_D exhibits a dip and then a rise as the angle θ_w decreases, approaching the value of the angle β (10^o). This rise can be explained by the fact that as θ_w approaches the value of β, the α particles which enter the port are neutralized more towards the pump duct opening at $z = z_{min}$; this increases their probability to escape to the pump duct. For the same reason, in addition to the rise of the current J_w with the angle β, the current J_D is expected to increase as β increases approaching the value of the angle θ_w. This increase is shown in Fig. 14.

6.2. *Dependence on the Plasma Parameters*

We consider a hydrogen plasma with the following geometric data: z_{max} = 25 cm, $F_A = 0.25$, $W_r = 2.1$ cm, $L_p = 1.575$ cm, $\theta_w = 90°$ and $\beta = 10°$. We study the dependence of the currents J_w and J_D on the plasma temperature, T, the ion flow speed, a, and the plasma density, n_p.

The current J_w is essentially the same as in the 1-D calculation, which was shown in Fig. 8. J_D versus T is shown in Fig. 15. The results show that the currents J_w and J_D increase as the plasma temperature decreases and become significant below 10 eV. The dependence on the ion flow speed, a, has been examined for three values of the angle β to check the influence of the perpendicular component of the velocity. As can be seen in Fig. 16, J_w increases considerably as the quantity $a \sin\beta$ increases. This can be explained, as in subsection 6.1, by the fact that increasing β leads to an increase in the ion velocity component perpendicular to the plate which causes more helium atoms to be backscattered towards the plate.

7. Conclusions

Transport of neutral helium in the low temperature region near divertor or limiter target plates has been studied using Monte Carlo techniques. As interactions with the plasma, helium atoms were assumed to undergo either electron impact ionization or elastic scattering by ions. We assume that the

ions have a shifted Maxwellian distribution with a drift velocity along the magnetic field. It was found that the scattering collisions cause a fraction of the helium atoms to be reflected back to the target plate. The neutral helium current scattered back to the plate increases as the plasma temperature decreases and becomes significant below 10 eV. Therefore, we can conclude that elastic scattering has a significant effect on the transport of neutral helium when the plasma temperature is below about 10 eV and this effect can be beneficial for the pumping of helium gas from the discharge chamber.

A 2-D code has been applied to the case where neutral helium atoms arise from the neutralization and reflection of α particles incident on a flat, vented target plate. We found that the neutral helium current scattered back to the target plate and the current escaping to the pump duct depend on the component of the ion flow velocity perpendicular to the plate. In addition, the current to the pump duct increases as the motion of the ions becomes more parallel to the port sides. The results show that the pumping of neutral helium can be increased by shortening and widening the ports, *e.g.*, for an ion temperature equal to 4 eV and with ports whose area equals 25% of the plate area, about 12% of the incident α particles can be pumped as neutral helium when the port length is about twice the width. Decreasing the angle between the magnetic field lines and the ports in the target plate significantly increases the amount of the helium atoms escaping to the pump duct. This is because the α particles impact the sides of the ports closer to the pump duct.

Acknowledgement

This research was supported by the Department of Energy under contract DE-FG02-86ER53218.

References

[1] BARR, W.L., *Fusion Technol.* **8** (1985) 1772.

[2] BARR, W.L., *private communications.*

[3] GOEDHEER, W.J., FOM-Instituut voor Plasmafysica, Rijnhuizen, Nieuwegein, The Netherlands, Rijnhuizen Report **84-153** (1984).

[4] POTTERS, J., and GOEDHEER, W., *Nucl. Fusion* **25** (1985) 779.

[5] SEKI, Y., SHIMOMURA, Y., MAKI, K., AZUMI, M., and TAKIZUKA, T., *Nucl. Fusion* **20** (1980) 1213.

[6] CUPINI, E., De MATTEIS, A., and SIMONINI, R., Commission of the European Communities, Directorate General XII-Fusion Programme-Brussels, report **EUR XII-324/9** (1983).

[7] HEIFETZ, D., POST, D., PETRAVIC, M., WEISHEIT, J., and BATEMAN, G., *J. Comput. Phys.* **46** (1982) 309.

[8] SAITO, S., SUGIHARA, M., FUJISAWA, N., UEDA, K., and ABE, T., *Nucl. Technol./Fusion* **4** (1983) 498.

[9] BELL, K.L., GILBODY, H.B., HUGHES, J.G., KINGSTON, A.E., and SMITH, F.J., *J. Phys. Chem. Ref. Data* **12** (1983) 891.

[10] HIRSCHFELDER, J.O., CURTISS, C.F., and BIRD, R.B., *Molecular Theory of Gases and Liquids*, **pp. 43 - 51**, John Wiley and Sons, Inc., New York (1964).

[11] BERNSTEIN, R., *Quantum Effects in Elastic Molecular Scattering*, Advances in Chemical Physics, **Vol. X**, edited by J. Ross, Wiley and Sons, New York (1966).

[12] GOLDSTEIN, H., *Classical Mechanics*, 2^{nd} edition, **pp. 105 - 114**, Addison-Wesley Publishing Company (1980).

[13] WOLNIEWICZ, L., *J. Chem. Phys.* **43** (1965) 1087.

[14] HELBIG, H.F., MILLIS, D.B., and TODD, L.W., *Phys. Rev.* **A2** (1970) 771.

[15] LINDHARD, L., SCHARFF, M., and SCHIOTT, H., *Math. Fys. Medd.* **33** (1963) 39.

[16] ECKSTEIN, W., and VERBEEK, H., in *Data Compendium for Plasma-Surface Interactions*, a **special issue** of *Nucl. Fusion* (1984) 12.

[17] BEHRISCH, R., and ECKSTEIN, W., in *Physics of Plasma-Wall Interactions in Controlled Fusion*, D. Post and R. Behrisch, Eds., Plenum, New York (1986) 413.

[18] KALOS, M.H., NAKACHE, F.R., and CELNICK, J., *Computing Methods in Reactor Physics* (H. Greenspan, C. N. Kelber and D. Okrent,

Eds.), **Chap. 5**, Gordon and Breach, New York (1968).

[19] HUGHES, M.H., and POST, D.E., *J. Comput. Phys.* **28** (1978) 43.

[20] CARTER, L.L., and CASHWELL E.D., **TID-26607**, *ERDA Critical Review Series* (1975).

[21] CASHWELL, E.D., and EVERETT, C.J., *A Practical Manual on the Monte Carlo Method for Random Walk Problems*, Pergamon Press, Inc., New York (1959).

(a)

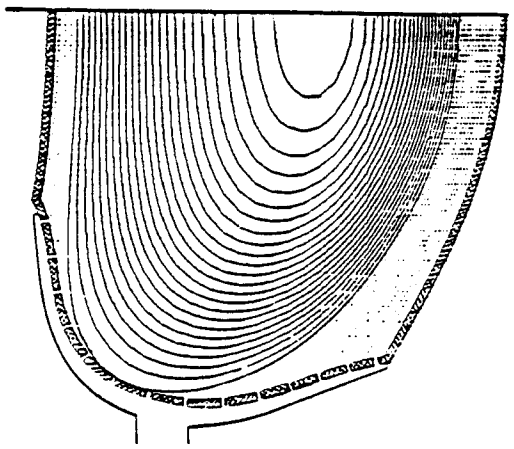

(b)

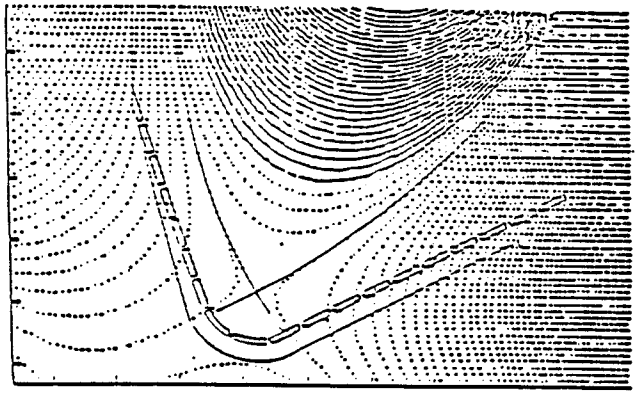

Figure 1: (a) Flat vented limiter plate, (b) Flat vented divertor plate.

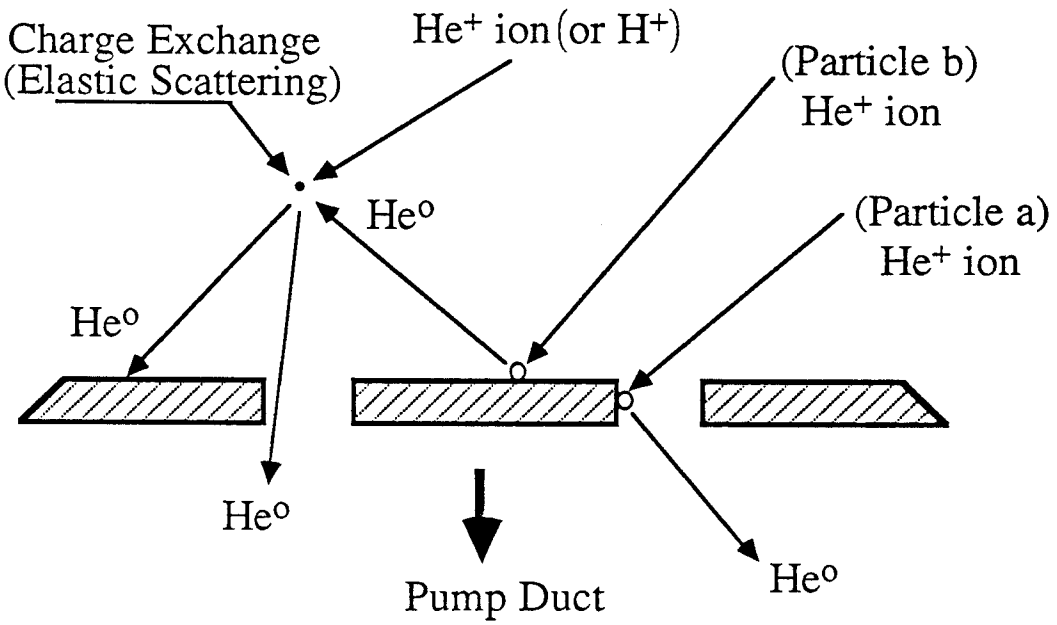

Figure 2: Recycling at the target plate.

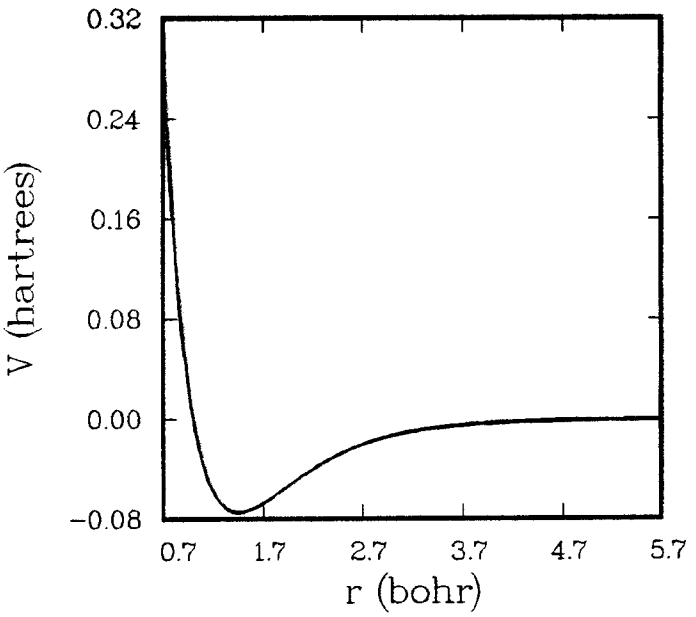

Figure 3: Wolniewicz potential versus proton-helium atom separation distance.

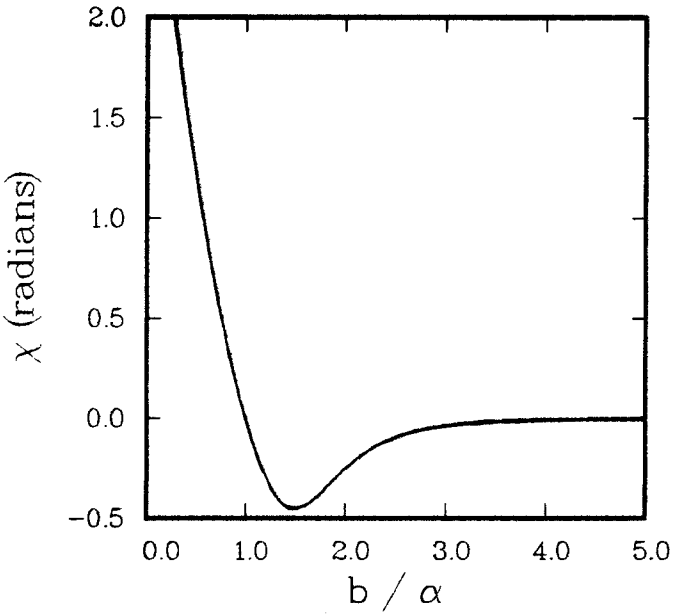

Figure 4: Classical deflection function versus normalized impact parameter (center of mass energy = 5.79567 eV).

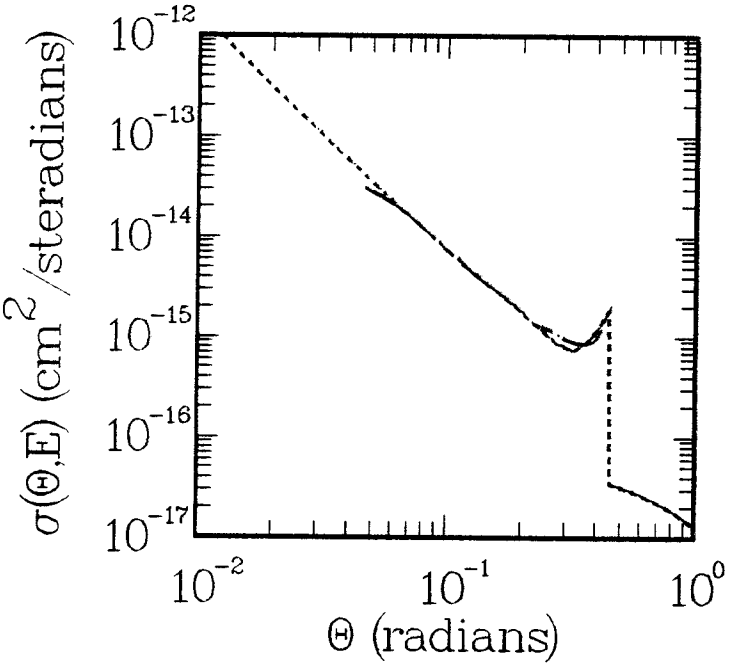

Figure 5: Classical differential elastic scattering cross section (center of mass energy = 5.79567 eV), – – – our results, — – — Helbig results.

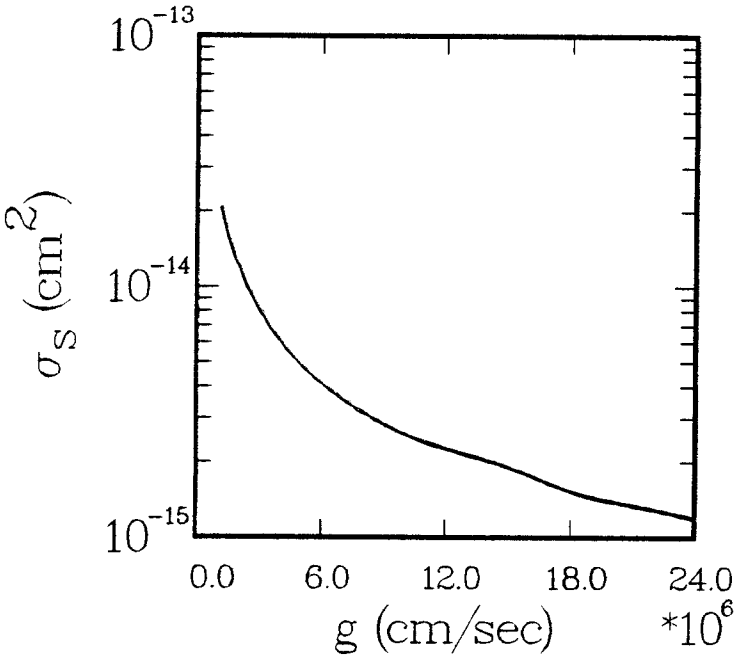

Figure 6: Total elastic scattering cross section versus helium-proton relative speed.

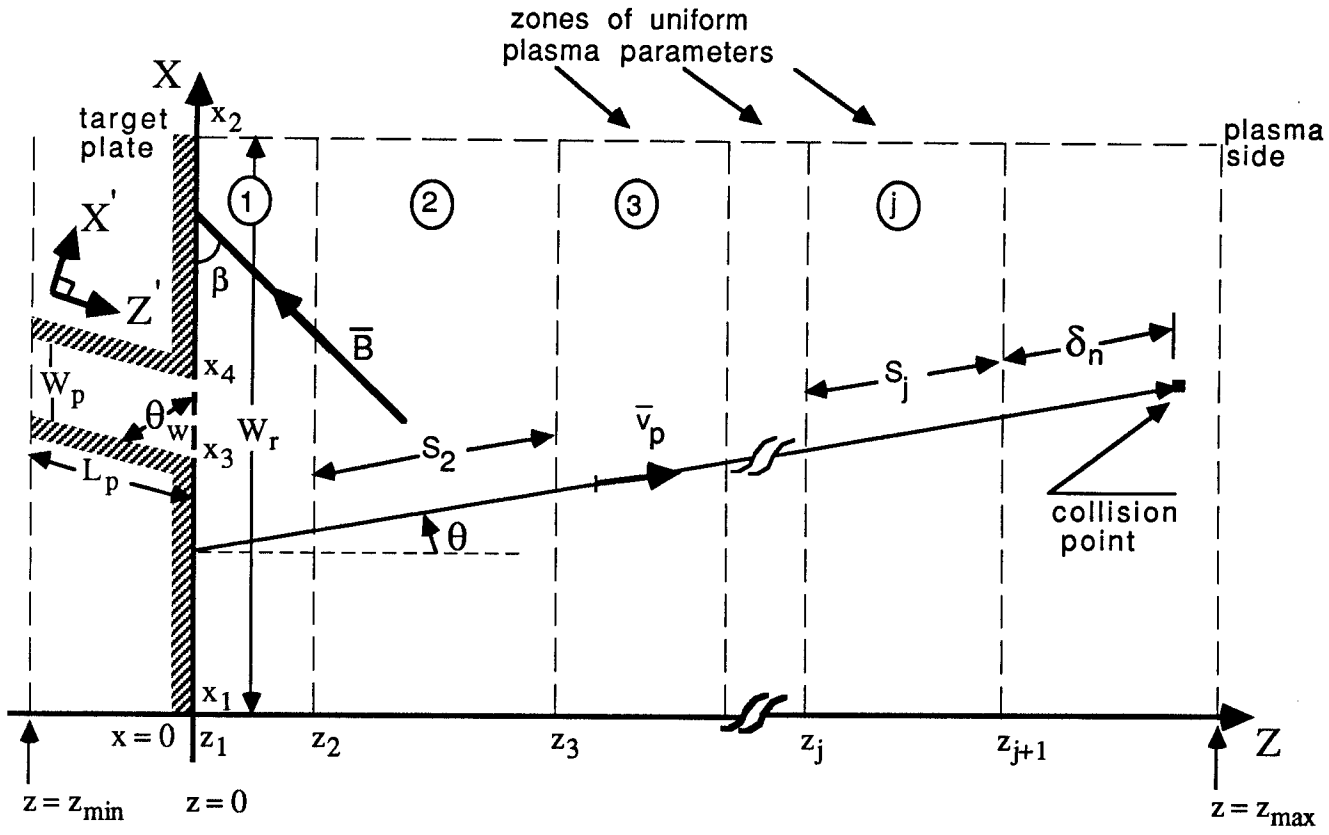

Figure 7: Geometry and coordinates .

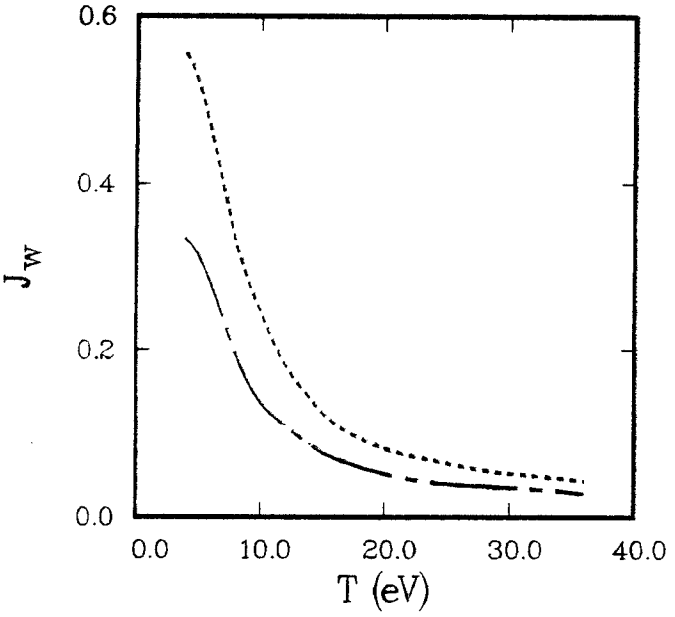

Figure 8: Neutral helium current to the plate versus temperature. (- - -) no reflection at the plate, (— - —) includes reflection at the plate.

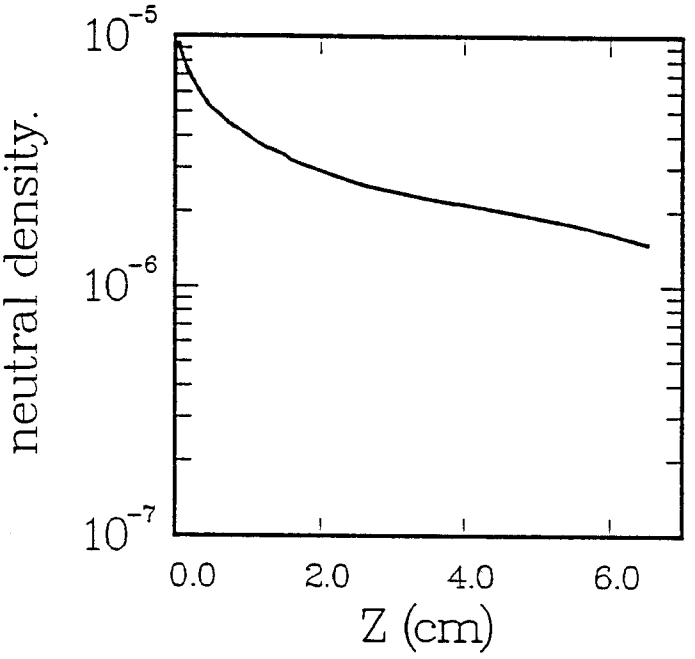

Figure 9: Neutral helium density versus distance from the target plate. Densities are normalized to one source particle/cm^2 s.

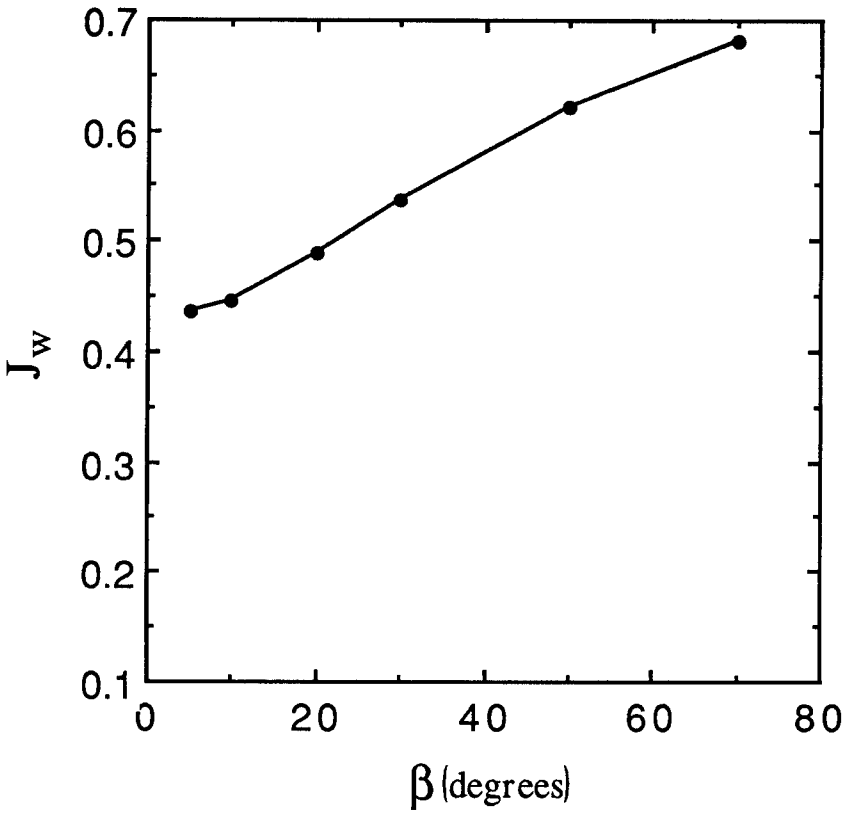

Figure 10: Neutral helium current to the plate versus β (z_{max} = 25 cm, $L_p = 1.575$ cm, $F_A = 0.25$ and $\theta_w = 90°$).

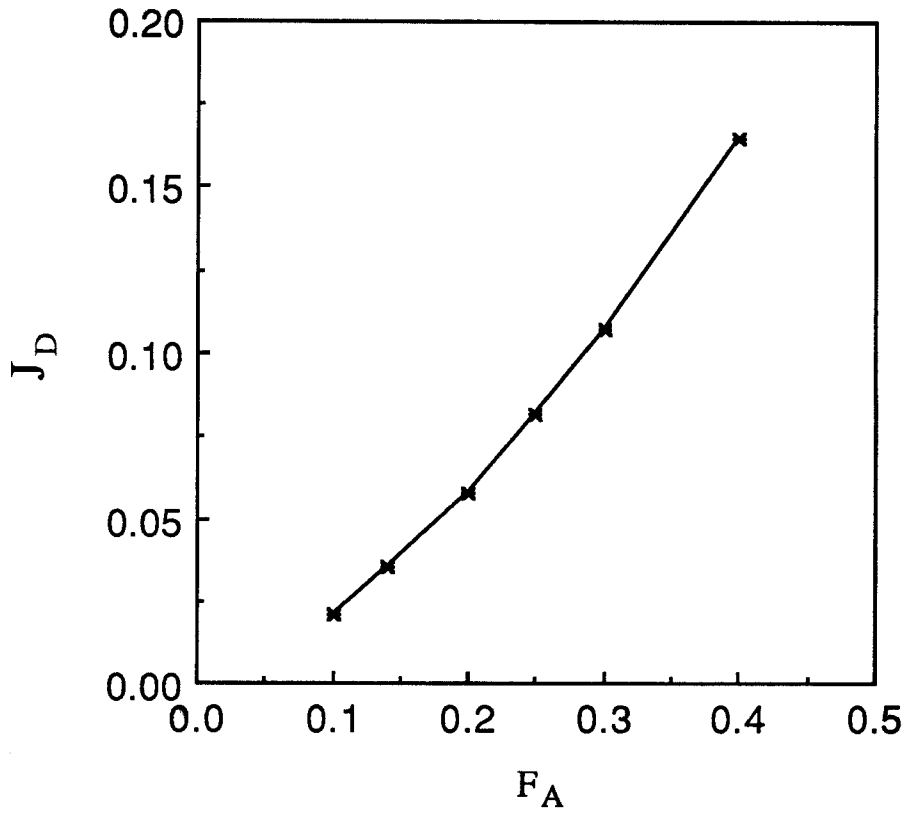

Figure 11: Neutral helium current to the pump duct versus F_A ($z_{max} = 25$ cm, $\theta_w = 90°$ and $\beta = 10°$).

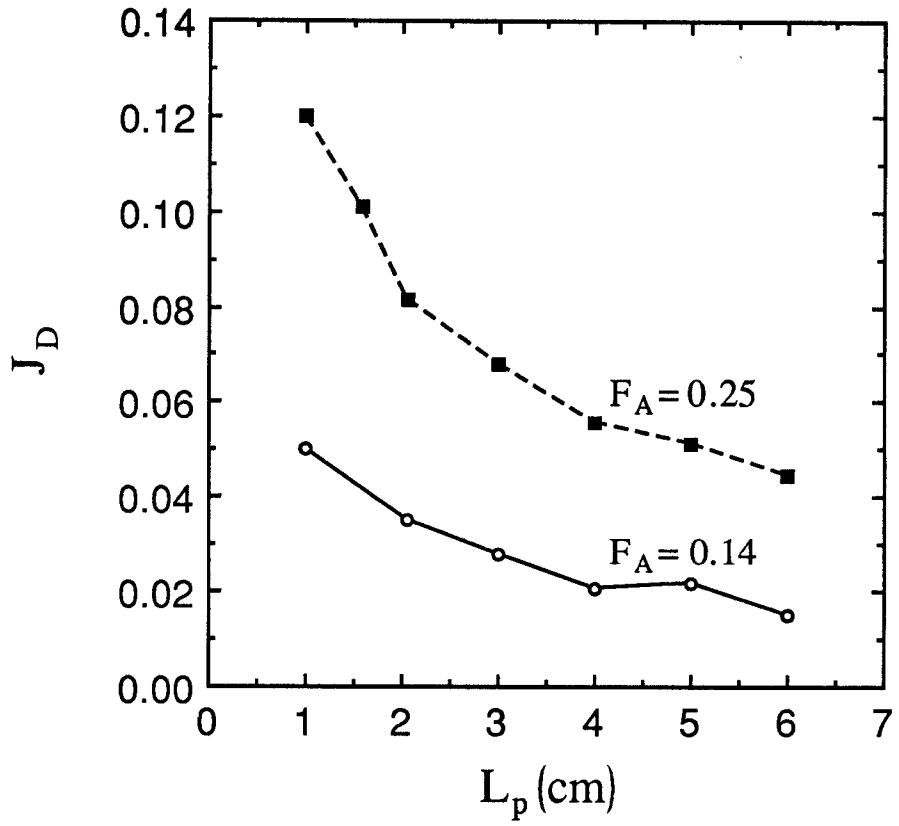

Figure 12: Neutral helium current to the pump duct versus L_p ($z_{max} = 25$ cm, $\theta_w = 90^o$ and $\beta = 10^o$).

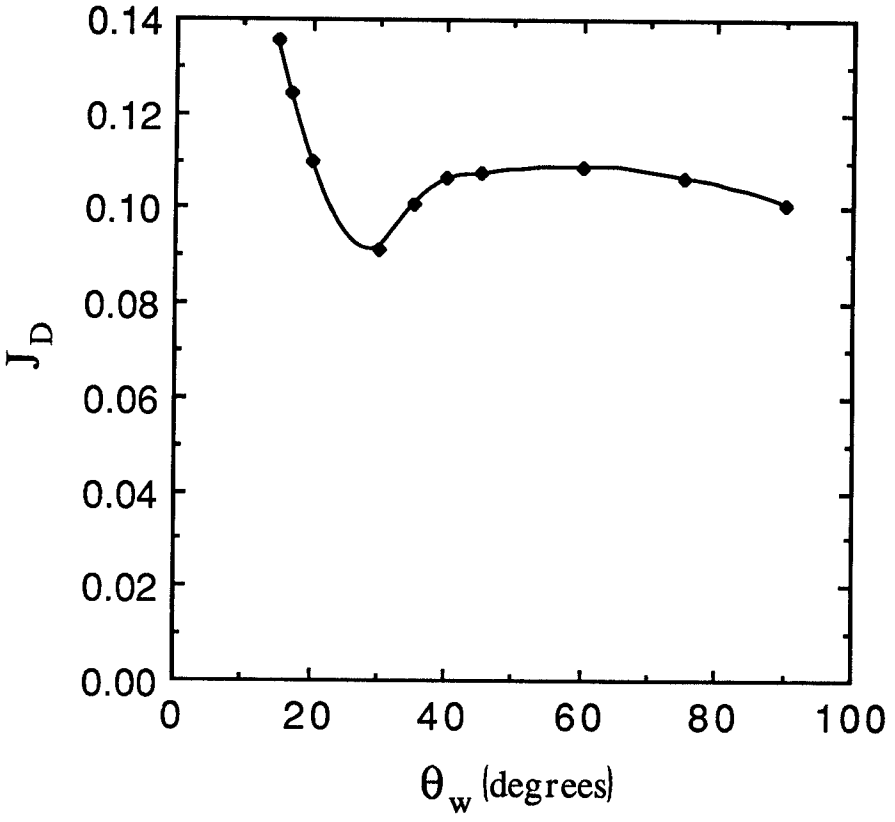

Figure 13: Neutral helium current to the pump duct versus θ_w (z_{max} = 25 cm, L_p = 1.575 cm, F_A = 0.25 and $\beta = 10°$).

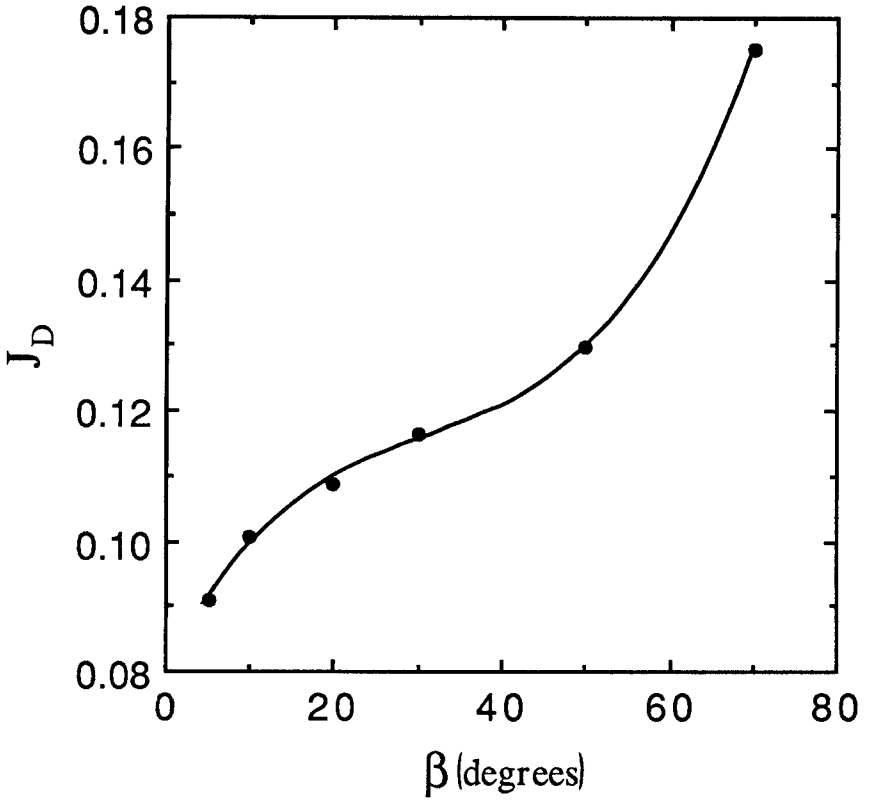

Figure 14: Neutral helium current to the pump duct versus β (z_{max} = 25 cm, L_p = 1.575 cm, F_A = 0.25 and θ_w = 90°).

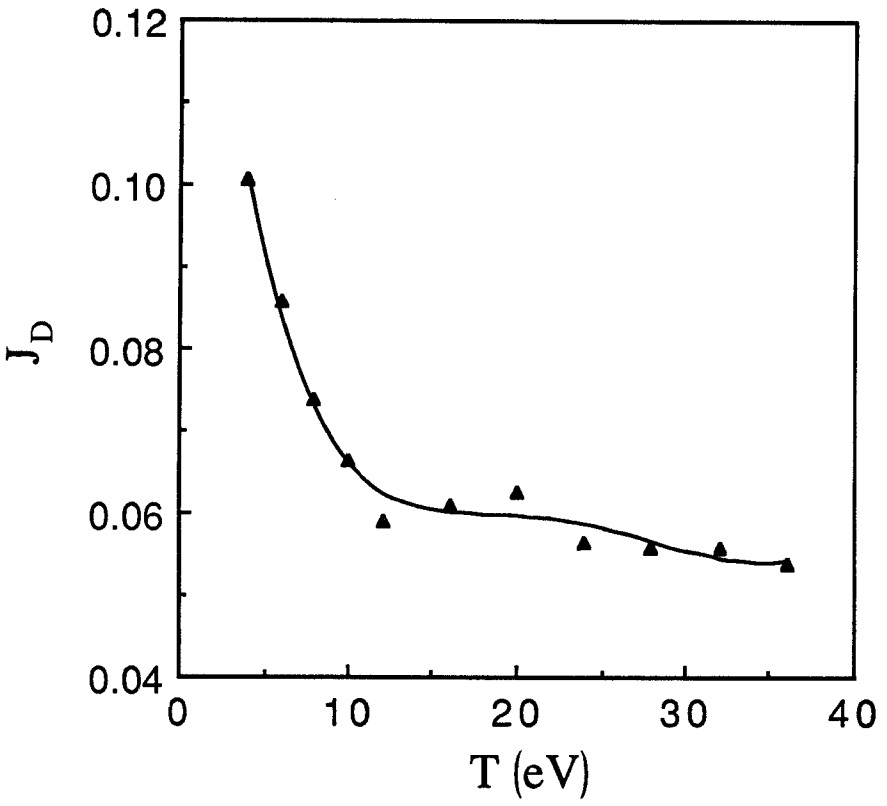

Figure 15: Neutral helium current to the pump duct versus T ($n_p = 1 \times 10^{14}$ cm^{-3}).

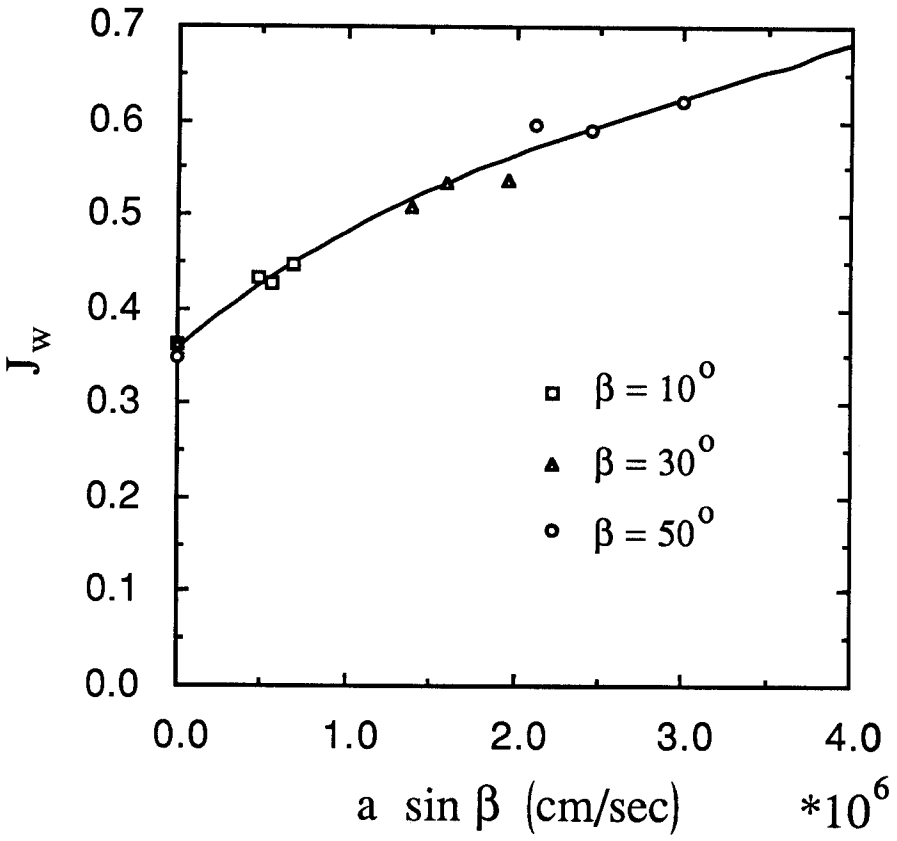

Figure 16: Neutral helium current to the plate versus $a \sin \beta$ ($n_p = 1 \times 10^{14}$ cm^{-3} and $T_i = 4$ eV).